Paper No. 281. (quote when citing this article)
Eleventh World Conference on Earthquake Engineering
ISBN: 0 08 042822 3

ASEISMIC PERFORMANCE OF REINFORCED CONCRETE 2-STORY VIADUCT

MOTOYUKI SUZUKI[1] and YOSHIO OZAKA[2]

1)Earthquake Engineering Division, Public Works Research Institute, Tsukuba City, 305, JAPAN
2)Department of Civil Engineering, Tohoku-Gakuin University, Tagajou City, 985, JAPAN

ABSTRACT

As many reinforced concrete(RC) viaducts have been used for traffic facilities as railway and highway bridges, it is very important to clarify the behavior of such structures during earthquake in order to establish a rational aseismic design method. The purpose of this study is to perform an elasto-plastic dynamic response analysis of RC 2-story viaduct in order to determine what type of factors effect the damage index of individual members as expressed by the ductility factor and accumulated plastic strain energy.

KEYWORDS

RC 2-story viaduct; dynamic response analysis; earthquake wave; damage index; ductility factor; accumulated plastic energy; aseismic design.

INTRODUCTION

The basic concept in present aseismic design of RC structures is expressed by the words: "Rational design is design which determines the yield strength of member such that its behavior will remain within the elastic region during a moderate earthquake that occurrs frequently, and which provides structures with plastic performance in order to absorb the energy input by a severe earthquake likely to occur only once in several tens of years(JSCE,1991)." As a result of extensive research on single column type-RC piers, design method for such structure has been established. Although many RC viaducts have been built for traffic facilities as railway and highway bridges, a rational seismic design for RC viaducts have not been established yet. The reasons are thought to be that they are statically indeterminate structure, and they display complex elasto-plastic behavior during big earthquake. Middle height beams are installed in RC 2-story viaducts to reduce the bending moment of the columns, and it is believed that the mechanical properties of these middle height beams substantially influence behavior of the entire structure(Suzuki et al.,1987). It is very important to clarify the behavior of such structures during earthquake in order to establish a rational aseismic design method. The purpose of this study is to perform an elasto-plastic dynamic response analysis of RC 2-story viaduct in order to determine what type of factors effect the damage index of individual members as expressed by the ductility and accumulated plastic energy.

ELASTO-PLASTIC DYNAMIC RESPONSE ANALYSIS METHOD

Equation of Motion

Generally, the earthquake response of a vibration system with multi−degree of freedom is expressed as the following equation.

$$[M]\{\ddot{y}\}+[C]\{\dot{y}\}+[K]\{y\}=-[M]\{\ddot{y}_0\} \tag{1}$$

Here, $[M]$, $[C]$, and $[K]$ represent the matrices which express the mass, damping and stiffness respectively. $\{\ddot{y}\}$, $\{\dot{y}\}$ and $\{y\}$ represent the vector of response acceleration, the response velocity and response displacement, and $\{\ddot{y}_0\}$ is the ground acceleration vector. In this analysis, RC 2−story viaduct at right angles to the bridge axis is analysed to solve eq. (1). Concerning the mass matrix, the mass was concentrated at the beam position at each level and half the mass of the adjacent columns was added to the mass of the beam. Mass equal to the mass of the bridge axis direction beams in one span was added to each level, and mass equal to the mass of the slab, roadway slab, and other parts of the superstructure in one span was added to the upper layer. Concerning the damping matrix, the initial damping used was the Rayleigh damping. And the damping factor $_sh$ was assumed to be 0.02 in both the first and secondary modes. And the numerical analysis was performed in succession using the linear acceleration method, and the time interval was set at 0.002 seconds.

Member Model

The member model used was the Giberson Model(Giberson et al.,1969) (see Fig. 1), it was modelled with rigid zones at the ends. Fig. 2 indicates a degrading tri−linear model which was used for this analysis.
The stiffness at unloading K_r is computed by the following formula(Suzuki et al.,1987).

$$K_r=K_y\ (\ \theta_{py}/\theta_{pmax}\ )^{0.4} \tag{2}$$

And the stiffness after yielding K_p is proportional to the yield stiffness K_y, and its proportional coefficient γ is discussed in the session of rigid frame analyzed.

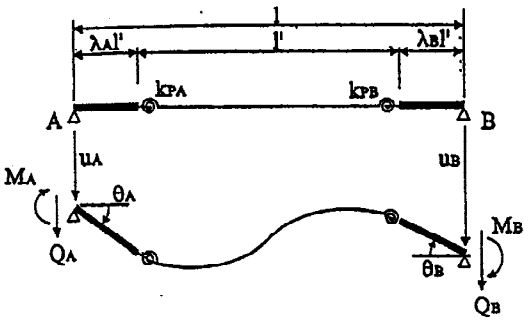

Fig. 1. Giberson model

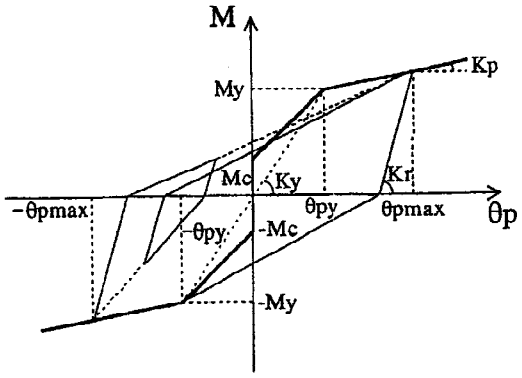

Fig. 2. Restoring force model

Energy Response

This research used the accumulated plastic deformation energy found from the energy response to evaluate accumulated damage. The following formula is obtained by multiplying both sides of eq. (1) by $\{\dot{y}\}^T$ and performing integration for the entire time an earthquake continues T(Housner,1959).

$$\int_0^T[M]\{\ddot{y}\}\{\dot{y}\}^T dt+\int_0^T[C]\{\dot{y}\}\{\dot{y}\}^T dt+\int_0^T[K]\{y\}\{\dot{y}\}^T dt=-\int_0^T[M]\{\ddot{y}_0\}\{\dot{y}\}^T dt \tag{3}$$

The right side expresses the total amount of energy input to the system by earthquake, while on the left side, the first term represents the kinematic energy, the second term represents the energy dispersed by the

damping W_h, and the third term represents the accumulated plastic deformation energy in the spring system W_P and the elastic deformation energy at the end of the earthquake. At the end of an earthquake, the elastic deformation energy is almost zero(Housner,1959), and in the end, the input earthquake energy is dissipated by the damping and the plasticization. For this analysis, it was assumed that the accumulated plastic deformation energy was expressed by accumulating the area of the hysteresis loop up to the end of the earthquake.

RC Viaduct

This study analyzes the direction at right angles to the axis of RC 2-story viaduct with a height of 12 m designed in conformity to Tohoku Shinkansen standard design(See Fig. 3). Its horizontal design seismic coefficient was 0.25, the column sections were 100cm×100cm at both the upper and lower stories, and the section of the middle height beam was 100cm×80cm. The axial reinforcement ratio ρ_t was 2.6% for the column and 1.8% for the middle height beam. Analyses were performed of seven rigid-frames, No.1 to No.7, by treating the yielding moment M_y and the yield stiffness K_y of the middle height beam as the variable factors(see Fig. 4). Although the stiffness after yield of the middle height beams is constant for all structures, the ratio of the stiffness after yield to the yield stiffness of the middle height beams γ varies between 0.017 (No.7) and 0.05 (No.1). And in all cases, the initial natural period was constant (primary natural period: 0.36 seconds, secondary natural period: 0.06 seconds), and the footing and top beams were provided with sufficient stiffness. Table 1 shows the material properties used for calculations.

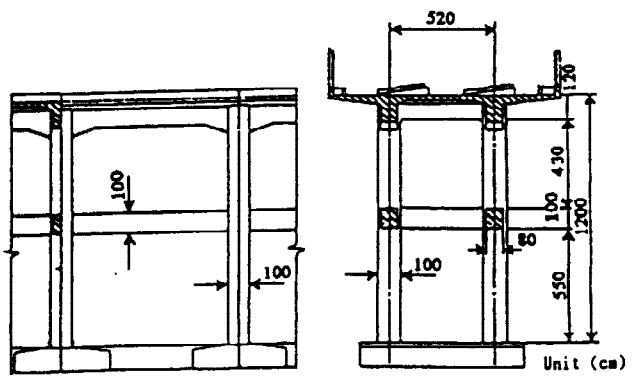

Fig. 3. 2-story RC viaduct for analysis

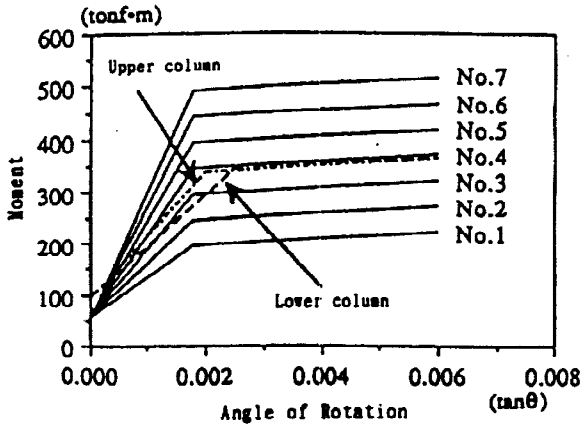

Fig. 4. Skelton curves of middle height beams

Table 1. Material properties

Concrete properties			
Compressive strength f_c (kgf/cm^2)	Tensile strength f_t (kgf/cm^2)	Strain at maximum stress ε_{co}	Ultimate strain ε_{cu}
270	35	0.002	0.0035

Steel reinforcement properties				
Yield strength f_y (kgf/cm^2)	Tensile strength f_u (kgf/cm^2)	Yield strain ε_y	Strain at beginning of strain hardening ε_{sh}	Ultimate strain ε_{su}
4,000	6,000	0.002	0.02	0.1

Yield Seismic Intensity

The first step was to find the yield seismic intensity when the rigid-plastic spring at each nodal point reaches yield moment. As shown in Fig. 5, when static load equivalent to the mass of each story is loaded in the horizontal direction on a rigid-frame model, a load expressed by the following formula is applied onto the first story.

$$P_1=\left(\frac{m_1}{m_2}\right)\cdot P_2 \tag{4}$$

Here:

m_1, m_2: Mass of each level

P_2:load applied onto the second levl

The yield seismic intensity for each nodal point is calculated by dividing the load when each nodal point has reached yield moment by the weight.

The method of preparing the member model and the overall stiffness matrix corresponds to the dynamic analysis method, and static incremental analysis was done by replacing analysis based on the equation of motion with an equilibrium equation. So the yield seismic intensity α_y of this nodal point was calculatedby dividing the load when each nodal point reached the yield moment by the weight.

$$\alpha_y=\frac{P_2}{(m_2 g)} \tag{5}$$

Here:

g: gravitational acceleration

Fig. 6 shows the changes in yield seismic intensity for each viaduct. This figure reveals that as the yield moment of the middle height beam (nodal point 5) rises, the yield seismic intensity of the bottom of the lower column (nodal point 1) and the top of the upper column (nodal point 4) increases, and the yield seismic intensity of the top of the lower column (nodal point 2) decreases. This indicates that the yield seismic intensity of the column is changed simply by changing the yield moment of the middle height beam by moment redistribution. And although, for viaduct No.1 to No.3, the value of the yield seismic intensity increases in the sequence, nodal point 5, 1, 4, 2, for viaduct No.4, values of nodal points 5 and 1 are reversed, and at viaduct No.7, values of nodal points 5 and 2 are reversed. And the values for the bottom of the upper column (nodal point 3) are all 2 or more.

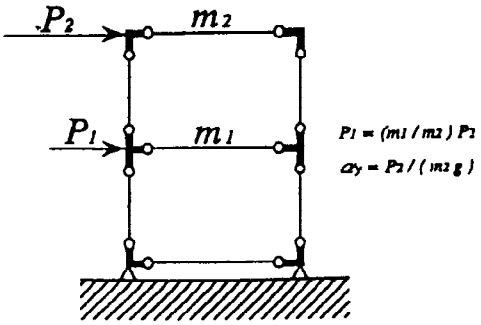

Fig. 5. Static monotonic loading

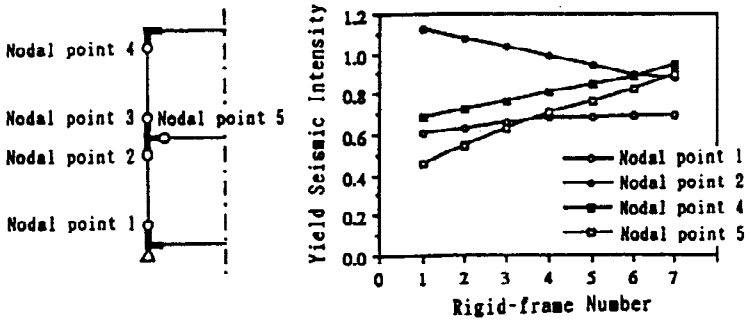

Fig. 6. Yield seismic intensity

Properties of the Input Seismic Waves

This study used the three seismic waves, that is El Centro(Imperial Valley Earthquake, 1940), Miyagi (Miyagi-ken Oki Earthquake, Sendai, 1978) and Tokachi(Tokachi Oki Earthquake, Hachinohe, 1986). Each duration is 30 seconds, each wave has a maximum acceleration between 0.4g and 0.8g, and was expanded or contracted as it was used. Fig. 7 shows the Fourier Spectrum. This figure reveals that the predominant period of the Miyagi-ken Oki Earthquake was at approximately 1.0 and 0.28 seconds and was at nearly 0.5 seconds for the El Centro Earthquake, but it is not clear for the Tokachi Oki Earthquake.

Fig. 8 shows the acceleration response spectrum for an elastic system with single degree of freedom. This figure shows that while the acceleration response amplification factor for the El Centro and Tokachi Oki earthquakes is a maximum of 4, it is smaller at 3 for the Miyagi-ken Oki Earthquake.

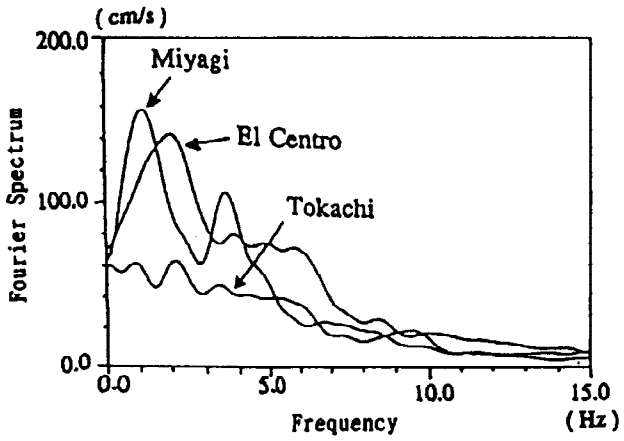

Fig. 7. Fourier spectrum of input seismic waves

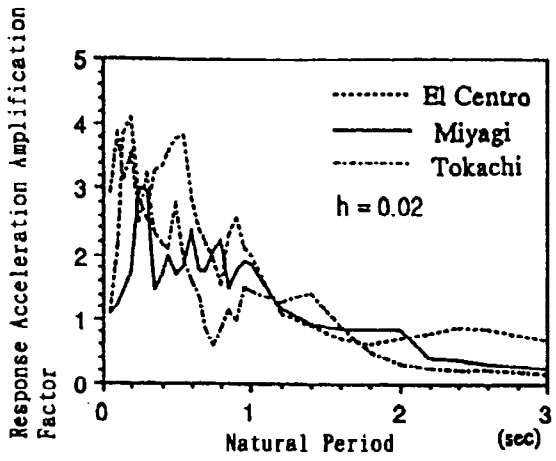

Fig. 8. Acceleration response spectrum

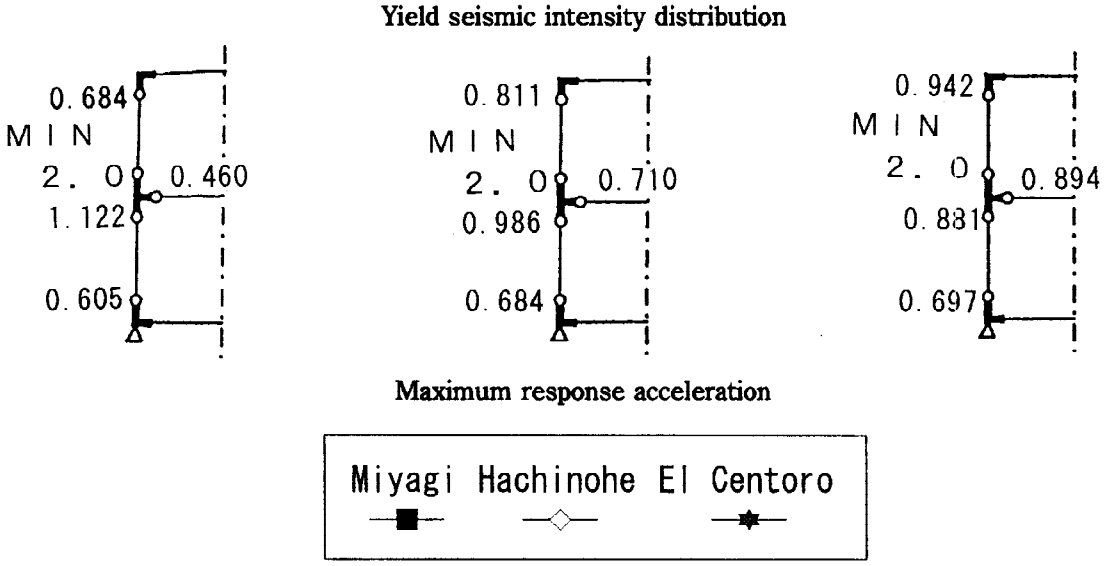

(1)Viaduct No.1 (2)Viaduct No.4 (3)Viaduct No.7

Fig. 9. Yield seismic intensity distribution and maximum response acceleration

ANALYSIS RESULTS

Maximum Response Acceleration

Fig. 9 shows maximum response acceleration α_{max} at the top of viaducts No.1, No.4, and No.7 obtained from

the elasto−plastic dynamic response analyses. These figures reveal that as the input seismic acceleration rises, the maximum response increases proportionally, but the amplification factor for the response acceleration to the input seismic wave actually declines. They also indicate that the maximum response value is the smallest for the Miyagi−ken Oki Earthquake, larger for the Tokachi Oki Earthquake, and largest for the El Centro Earthquake. It is possible to speculate that these results occurred for the following reason: because the primary natural period of a viaduct is 0.36 seconds, the response acceleration amplification produced by the El Centro Earthquake, the Tokachi Oki Earthquake, and the Miyagi−ken Oki Earthquake, are 3, 2.3, and 1.8 on the basis of the acceleration response spectrum for elastic system with a single degree of freedom(see Fig. 6).

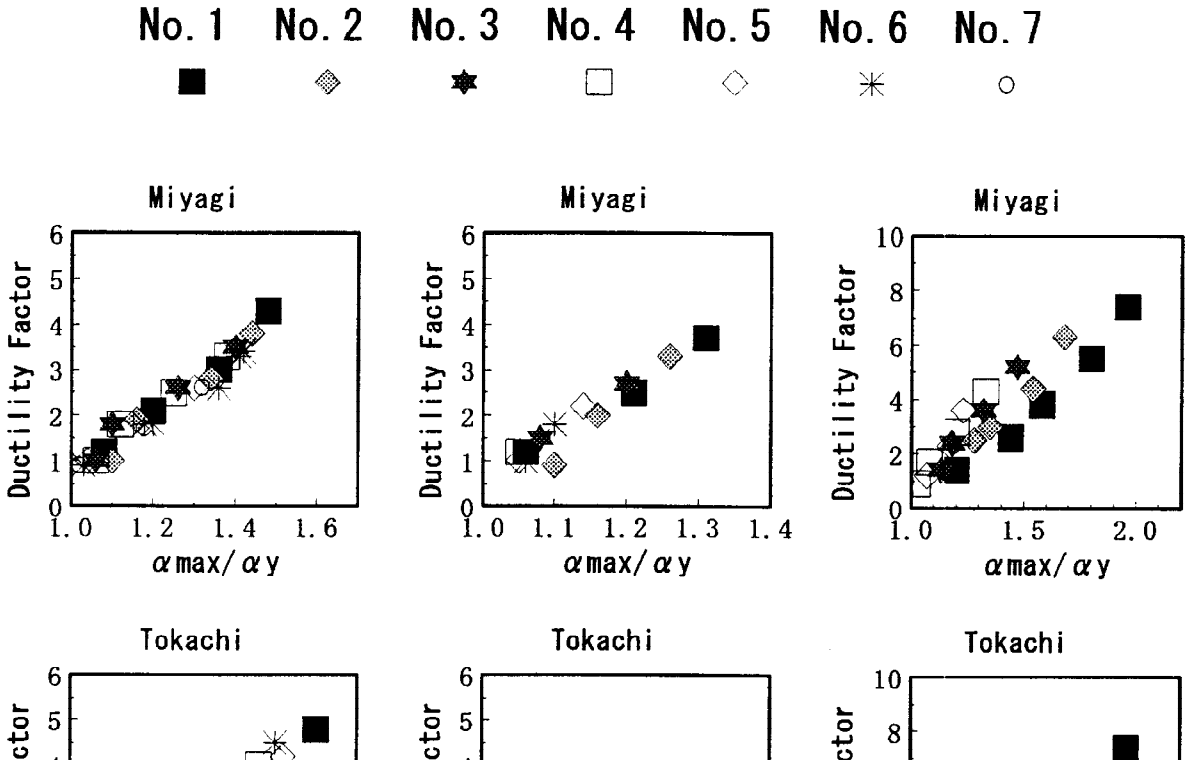

Next, the results of all viaducts show that the greater the yield moment M_y of the middle height beams, the larger the maximum response acceleration. This is a result of the fact that the acceleration response amplification factor rises as M_y of the middle height beams rises, because the yield seismic intensity of the overall structure rises.

Ductility Factor – Maximum Response Acceleration

Fig. 10 shows the relationship between the damage index of a viaduct and the maximum response acceleration. The axis of abscissa is the ratio of the maximum response acceleration at the top of each viaduct to the yield seismic intensity of individual members (α_{max}/α_y), and the axis of ordinates is the ductility factor μ ($\theta_{pmax}/\theta_{py}$) as an index expressing the damage index. These figures show that at nodal points 1 and 4 whose skeleton

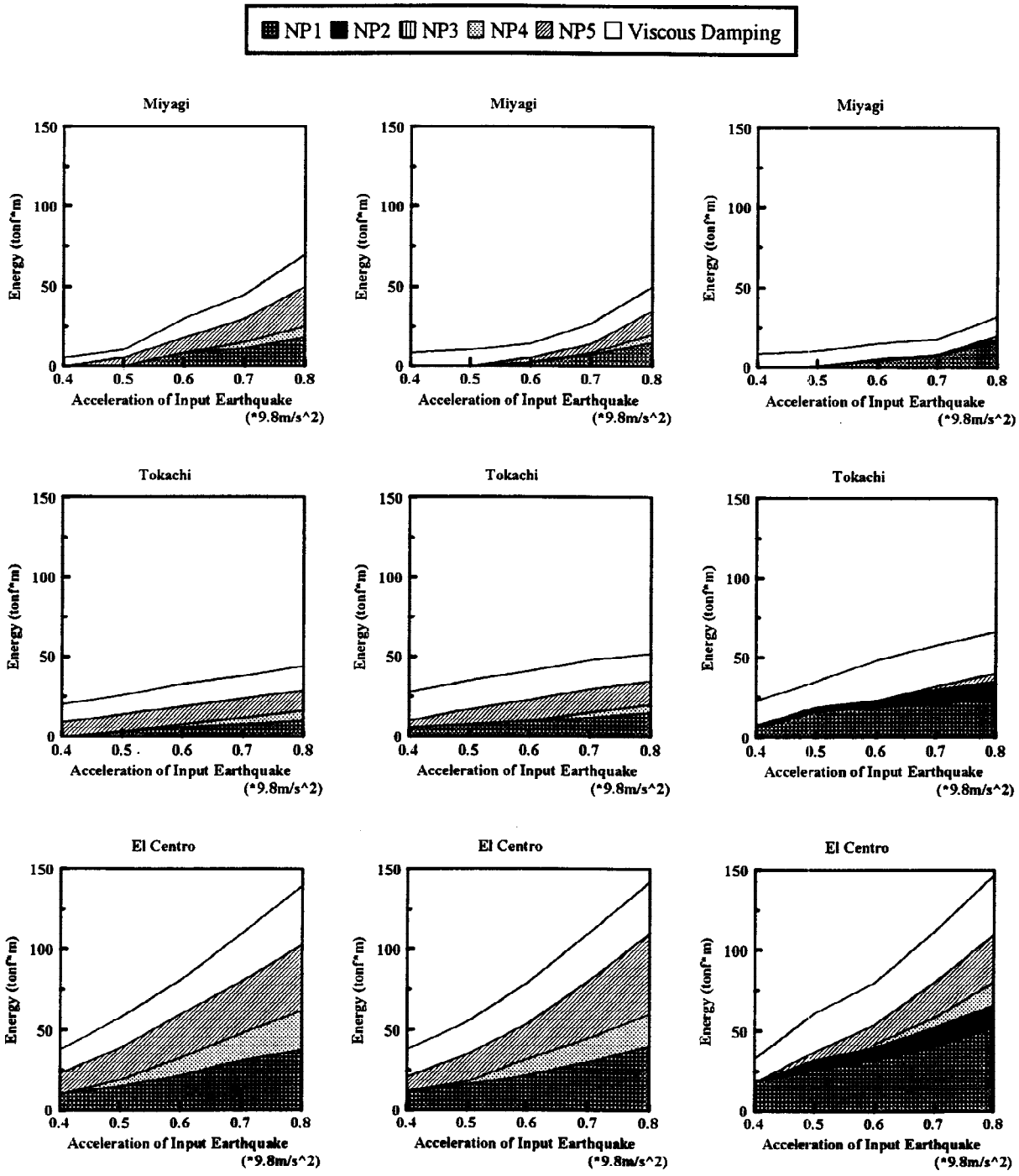

(1)Viaduct No.1 (2)Viaduct No.4 (3)Viaduct No.7

Fig. 11. (1) to (3) Distribution in the accumulated plastic deformation energy

curves are identical, little scattering is produced by the rise in the yield moment of the middle height beams, and that there is little difference between the seismic waves.

Accumulated Deformation Energy

Fig. 11 (1) to (3) shows distribution in the accumulated plastic deformation energy according to the input earthquake's maximum acceleration. The white areas in the figures represent the difference between the total input energy E and the accumulated plastic deformation energy W_P and therefore correspond to the energy based on viscous damping W_h. And the accumulated energy at each nodal point is the energy of two rigid−plastic springs.

In areas where the input earthquake acceleration is small, a great deal of energy is absorbed by viscous damping, but as the earthquake acceleration increases, the proportion absorbed by the accumulated plastic energy rises. And this reveals that in the case of viaducts whose yield seismic intensity is lower at nodal point 2 than at nodal point 5, in other words, No.7 viaduct where there is a possibility of the top of the lower column yielding before the middle height beams, the black zone is large.

In No.1, when the maximum input acceleration is small, the proportion of energy absorbed by the middle height beam is large. But as the earthquake acceleration increases, the amount of energy absorbed by the column grows. As the ductility at nodal point 5 is greater than ductility at nodal point 1, the middle height beam should

suffer greater damage. This is believed to occur because the shape of the skeleton has a greater effect than the accumulation of energy. In other words, the larger the skeleton, that is, the larger the yield moment M_y, the higher the absolute value of the energy when the ductility is equal. This suggests that it is impossible to judge the damage based solely on the absolute value of the energy.

RESULTS

The purpose of this study was to investigate the influence of the strength of the middle height beams and the properties of seismic waves on the behavior of RC 2−story viaduct in order to establish a rational aseismic design method for such structure. In brief, elasto−plastic dynamic response analysis was performed at the member level on RC 2−story viaduct to assess the damage suffered by each member from two points of view: ductility and accumulated plastic deformation energy. The following conclusions were made based on the analysis.

(1) The maximum response acceleration of an elasto−plastic structure subjected to seismic motion can be predicted based on the elastic system response spectrum and the yield seismic intensity of each member.
(2) There is a close relationship between the maximum response acceleration and the damage to each member, and the level of the damage varies widely under the influence of the stiffness after yield ratio γ.
(3) The accumulated plastic deformation energy displays tendencies that vary considerably, not only in response to the properties of the response spectrum and to the yield seismic intensity of each member, but according to the repetition properties of the seismic waves.
(4) A study of damage to the members of a viaduct revealed that from the point of view of the failure process, it was better for the middle height beam to yield before the columns.

REFERENCES

Giberson, M.F.(1969). Two nonlinear beams with definition of ductility, ASCE, 95ST2, 137−157.
Housner, G.W.(1959). Behavior of structures during earthquakes, ASCE, EM 4, 109−129.
Japan Society of Civil Engineers(1991). Concrete standards and guidelines (Design Volume).
Suzuki, M., Takeyama, Y., Kikuchi, H., Ozaka, Y.,(1987). Analysis of damages inflicted on reinforced concrete viaducts during the Miyagiken oki earthquake, Proceedings of the Japan Society of Civil Engineers, 384,43−52.